Collision-Induced Absorption of CH_4-CO_2 and H_2-CO_2 Complexes and Their Effect on the Ancient Martian Atmosphere

Paul J. Godin[1], Ramses M. Ramirez[2,3], Charissa Campbell[1], Tyler Wizenberg[4], Tue Giang Nguyen[1], Kimberly Strong[4], John E. Moores[1]

[1]Department of Earth and Space Science and Engineering, York University, 4700 Keele Street, Toronto, Ontario, M3J 1P3, Canada
[2]Earth-Life Science Institute, Tokyo Institute of Technology, 2-12-1-IE-1 Ookayama, Meguro-ku, Tokyo, 152-8550, Japan
[3]Space Science Institute, 4765 Walnut St, Suite B, Boulder, CO 8030, USA
[4]Department of Physics, University of Toronto, 60 St. George Street, Toronto, Ontario, M5S 1A7, Canada

Key Points:

- First temperature-dependent experimental measurements of CO_2-H_2 and CO_2-CH_4 CIA cross-sections
- Radiative transfer calculations of the early Mars atmosphere were performed using the newly acquired CIA cross-sections
- Surface temperatures above 273 K can be reached if surface pressures exceed 3 bar for 10% CH_4 or 2 bar for a 5% H_2 atmosphere

Corresponding author: Paul J. Godin, pgodin@yorku.ca

Abstract

Experimental measurements of collision-induced absorption (CIA) cross-sections for CO_2-H_2 and CO_2-CH_4 complexes were performed using Fourier transform spectroscopy over a spectral range of 100-500 cm^{-1} and a temperature range of 200-300 K. These experimentally derived CIA cross-sections agree with the spectral range and temperature dependence of the calculation by Wordsworth et al. (2017), however the amplitude is half of what was predicted. Furthermore, the CIA cross-sections reported here agree with those measured by Turbet et al. (2019). The CIA cross-sections can be applied to planetary systems with CO_2-rich atmospheres, such as Mars and Venus, and will be useful to terrestrial spectroscopists.

Additionally, radiative transfer calculations of the early Mars atmosphere were performed and showed that CO_2-CH_4 CIA would require surface pressure greater than 3 bar for a 10% methane atmosphere to achieve 273 K at the surface. CO_2-H_2, however, liquid water is possible with 5% hydrogen and less than 2 bar of surface pressure.

Plain Language Summary

Temperature-dependent experimental measurements of collision-induced absorption (CIA) cross-sections for CO_2-H_2 and CO_2-CH_4 complexes were measured for the first time over a spectral range of 100-500 cm^{-1} and a temperature range of 200-300 K. These experimentally derived CIA cross-sections are half as strong as what was predicted by Wordsworth et al. (2017), but agree with those measured by Turbet et al. (2019), strengthening our confidence in these results. The CIA cross-sections can be applied to planetary systems with CO_2-rich atmospheres, such as Mars and Venus, and will be useful to terrestrial spectroscopists. Additionally, simulations of the early Mars atmosphere were performed and showed that a surface pressure greater than 3 bar for a 10% methane atmosphere or 5% hydrogen and less than 2 bar of surface pressure to achieve liquid water at the surface of Mars.

1 Introduction

Geological evidence suggests that there was once liquid water on ancient Mars (Ramirez & Craddock, 2018; Craddock & Howard, 2002; Mangold et al., 2004; Stepinski & Stepinski, 2005; Barnhart et al., 2009; Hynek et al., 2010; Matsubara et al., 2013); this leads to an unanswered question of how could the early Martian atmosphere have maintained a greenhouse effect sufficient to allow for water on the surface present as a liquid? Ramirez et al. (2014) proposed the idea that collision-induced absorption (CIA) between carbon dioxide (CO_2) and hydrogen gas (H_2) from volcanic events could provide the additional atmospheric absorption needed to trap enough radiation to raise the ancient Martian surface temperature above freezing. However, there were no measured CO_2-H_2 CIA cross-sections available in the literature at the time of Ramirez et al. (2014), so N_2-H_2 was used as a proxy, but they had argued that CO_2-H_2 CIA should be stronger. This was followed up in a study by Wordsworth et al. (2017), wherein they simulated the CIA of CO_2-H_2 and CIA of CO_2 and methane (CH_4), and their simulations did show that CO_2-H_2 CIA was stronger than N_2-H_2 CIA. Wordsworth et al. (2017) derived their CIA by performing *ab initio* calculations of the zeroth spectral moment of a CO_2-H_2/CH_4 system, and then approximating the spectra as a linear combination of CO_2-CO_2 and H_2-H_2 or CH_4-CH_4 CIAs with the weighting determined by the *ab initio* calculation. The theoretical cross-sections from Wordsworth et al. (2017) have strong absorption features in the range of 0-600 cm^{-1} and 1200-1500 cm^{-1} for CO_2-CH_4; for CO_2-H_2, absorption was predicted to be a broad feature over the range of 0-1500 cm^{-1}. While this approximation appears to give accurate results, there can be significant deviations. For example, for CO_2-CH_4 above 1000 cm^{-1}, there are no CH_4-CH_4 CIA cross-sections in the literature, so a linear combination ends up simply as scaled CO_2-CO_2 CIA cross-section. For these reasons,

experimental validation of this linear combination approximation method are still required (Karman et al., 2019).

Additional modeling by Ramirez (Ramirez, 2017) used the cross-sections from Wordsworth et al. (2017) in more sophisticated Martian climate models and found that the inclusion of CIA between CO_2 and H_2 does result in a warm and wet early Mars that agrees with the paleopressure and climate stability constraints with only 1% hydrogen concentrations. Unfortunately, computing CIA cross-sections is quite challenging, and to date, the only CIA cross-sections for CO_2-H_2 and CO_2-CH_4 complexes in the literature are limited to room temperature, a spectral range of 60 to 535 cm^{-1}, and a resolution of 1 cm^{-1} (Turbet et al., 2019); which found that the experimentally derived CIA cross-sections are weaker than predicted by Wordsworth et al. (2017), but still stronger than N_2-H_2 CIA.

This paper expands upon the experimental work of Turbet et al. (2019), detailing the first temperature-dependent experimental measurements of CO_2-H_2 and CO_2-CH_4 CIA. Given that experimentally derived CIA cross-sections are more reliable than predicted ones, these new experimentally derived cross-sections are used in early Mars climate models to improve our understanding of the impact CIA may have had on the climate of ancient Mars.

2 Laboratory Measurements of Collision-Induced Absorption

2.1 Experimental Procedure and Data Analysis

Experiments were performed at the Far-IR beamline of the Canadian Light Source (CLS) Synchrotron facility. The IR absorption spectra were obtained using a Bruker IFS 125HR Fourier transform spectrometer connected to a temperature-controllable White-type cell with a pathlength of 7275 ± 6 cm. Experiments were performed using a globar source, mylar beamsplitter, polypropylene windows, and Si bolometer detector. Spectra were recorded at an unapodized resolution of 0.05 cm^{-1} (maximum optical path difference of 20 cm). Each measurement consisted of 300-500 co-added spectra. Temperature control was provided by a recirculating chiller. The chiller was capable of reaching temperatures as low as 203 K with the cell containing gas at atmospheric pressure.

The gas samples were commercial products from Praxair with stated high purities of greater than 99%. The cell was evacuated using a Varian turbo pump. The pressure in the gas cell was measured using a combination of a 10 and 1000 Torr MKS baratron pressure gauges. At each temperature, measurements were made at two pressure combinations as detailed in Table 1. Empty cell scans were performed between filled cell runs to monitor baseline stability. Due to safety limitations when using explosive gases at the CLS, the mixing ratio of H_2 in CO_2 was restricted to a maximum 8.3%; while for CH_4 in CO_2, the mixing ratio was restricted to maximum 20%. Methane experiments were performed by first filling the cell with methane, followed by adding CO_2. The H_2 experiments were performed using pre-mixed H_2-CO_2 gas cylinders as indicated in Table 1.

The absorption of light by a medium at a given pressure and temperature (P, T) can be described by the well-known Beer-Lambert Law:

$$I(\tilde{\nu}) = I_o(\tilde{\nu})e^{-\chi(\tilde{\nu})} \quad (1)$$

where $I(\tilde{\nu})$ is the intensity at wavenumber $\tilde{\nu}$ after passing through the gas sample (filled-cell measurement) and $I_o(\tilde{\nu})$ is the incident intensity (empty-cell measurement). $\chi(\tilde{\nu})$ is the optical depth, which for a mixture of CO_2 and another gas in a cell is given by:

$$\begin{aligned}\chi(\tilde{\nu}) = {} & L(\rho_{CO_2}\sigma_{CO_2}(\tilde{\nu}) + \rho_x\sigma_x(\tilde{\nu}) \\ & +\rho^2_{CO_2}\sigma_{CO_2+CO_2}(\tilde{\nu}) + \rho^2_x\sigma_{x+x}(\tilde{\nu}) \\ & +\rho_{CO_2}\rho_x\sigma_{CO_2+x}(\tilde{\nu}))\end{aligned} \quad (2)$$

Table 1: Summary of experimental conditions for CIA experiments with CO_2 and CH_4 or H_2.

Temperature (K)	**Total Pressure (Torr)**	**CH_4 Pressure (Torr)**	**% H_2**
293.80±0.05	750.1±0.08	156.5±0.05	0
293.40±0.05	762.5±0.15	76.7±0.05	0
250.10±0.05	743.6±0.11	152.0±0.06	0
250.15±0.08	687.0±0.12	80.1±0.05	0
204.05±0.08	751.0±0.17	150.7±0.06	0
203.20±0.05	760.4±0.30	75.8±0.06	0
292.60±0.05	745.3±0.31	0	4.009
293.12±0.06	742.4±0.13	0	8.312
250.01±0.05	718.1±0.33	0	4.009
250.45±0.15	741.7±0.44	0	8.312
203.30±0.05	756.4±0.19	0	3.987
203.50±0.05	757.5±0.25	0	8.270

where L is the cell length, ρ is the density of the gas, and $\sigma(\tilde{\nu})$ are the absorption cross-sections for either single gas species or CIA of mixed species depending on the subscript (x designating either H_2 or CH_4). The density of a gas in the cell is related to the pressure by:

$$\rho_x = \frac{P_x T_o}{P_o T} N_L \tag{3}$$

where P_o and T_o are standard conditions for pressure and temperature, and N_L is Loschmidt's constant.

Single gas species absorption cross-sections exist in the literature for CH_4, H_2, and CO_2 (Gordon et al., 2017); while CIA cross-sections exist for CO_2-CO_2 (Gruszka & Borysow, 1997), CH_4-CH_4 (Borysow & Frommhold, 1987), and H_2-H_2 (Abel et al., 2011) at the temperatures and spectral region investigated in this study. The absorption effects from single gas species, CO_2-CO_2 CIA, CH_4-CH_4 CIA, and H_2-H_2 CIA are simulated using the HITRAN Application Programming Interface (HAPI) (Kochanov et al., 2016). These absorption effects are then subtracted from the optical depth. Additionally, there was some water contamination in the cell, which requires the subtraction of water absorption lines from the measured optical depth; however, since the concentration of water is unknown, the optical depth was fit to match the absorption spectra of water in contaminated regions, using the density of water as a free parameter. The removal of these unwanted absorption features is not perfect, since there are small differences between the simulated lines from HAPI and the measured spectra. A 7 cm^{-1} median filter was applied to remove any remaining narrow features. Lastly, the baseline was adjusted to account for fluctuations in light intensity between empty- and full-cell measurement runs. Wavenumbers of known zero optical depth are used to fit a linear baseline to the spectra.

Once the optical depth has been cleaned of the unwanted absorption effects, the CIA absorption cross-sections can be found via a linear fit of optical depth versus pres-

sure for a given temperature and wavenumber. All fits have a forced convergence of $\chi = 0$ for $P = 0$, with

$$\chi(\tilde{\nu}) = \frac{P_x T_o}{P_o T} N_L L \sigma(\tilde{\nu}). \quad (4)$$

Sources of error include subtraction of unwanted absorption features (10%), temperature fluctuations (±0.2 K), baseline adjustment (10%), and pressure readout (±0.08 Torr). These errors are propagated in the calculation of the optical depth to determine its uncertainty. The uncertainty of the optical depth is used to assign weights in the linear fit against pressure to find the absorption cross-section. The final uncertainty is the sum, in quadrature, of the linear fit error, pathlength uncertainty (±6 cm), and sample purity error (±1.0%), expressed at the 3σ confidence interval.

2.2 Collision-Induced Absorption Cross-sections

Measured CO_2-CH_4 and CO_2-H_2 CIA cross-sections as a function of temperature are shown in Figures 1 and 2, respectively. Below 100 cm^{-1}, the limit of the detector begins to be reached and the amplitude of the cross-section becomes less reliable; above 500 cm^{-1}, CO_2 lines begin to saturate the detector, preventing the detection of other types of absorption.

At room temperature, the measurement from this work for CO_2-CH_4 CIA agree with the experimental results from Turbet et al. (2019), and its observed that the theoretical prediction of Wordsworth et al. (2017) overestimates the CIA by roughly a factor of 2. Looking at the temperature dependence of the CIA, the predicted increase in strength with decreasing temperature is also observed. Once again, Wordsworth et al. (2017) overestimates the CIA by roughly a factor of 2 at these colder temperatures.

Similar results are observed in the CO_2-H_2 CIA measurements, as seen for CO_2-CH_4, although the uncertainty in the derived CIA is larger overall. Due to the experimental safety limitations on the amount of hydrogen gas permitted in the gas cell, it was difficult to resolve the CO_2-H_2 CIA from the noise, especially at higher temperatures where the CIA effect is weaker, hence the uncertainty is higher compared to the CO_2-CH_4 CIA measurements. Despite this, an overestimation factor of 2 can still be inferred when comparing the prediction from Wordsworth et al. (2017) to the experimental measurements, including the measurement by Turbet et al. (2019).

Ultimately, these results agree with the prediction of Wordsworth et al. (2017) when it comes to the spectral range, and temperature dependence. However, the Wordsworth et al. (2017) prediction consistently overestimates the strength of the CIA by a factor of 2. At room temperature, these results agree within combined errors with the experimental cross-sections of Turbet et al. (2019), strengthening our confidence in those numbers. There appears to be more internal structure in the CIA cross-sections reported in this work compared to those of Turbet et al. (2019). This may be due to the increased resolution of this experiment or residual of incompletely removed unwanted absorption lines.

Attempts were also made to observe the CIA above 500 cm^{-1}, using an MCT detector and KBr windows/beamsplitter. However in this regime, absorption lines from CO_2 and CH_4 were so strong that in order to not saturate the detector, less than 0.05 Torr of those gas species was used. With such a small amount of gas present, there was no longer enough to produce a measurable CIA signal above the noise.

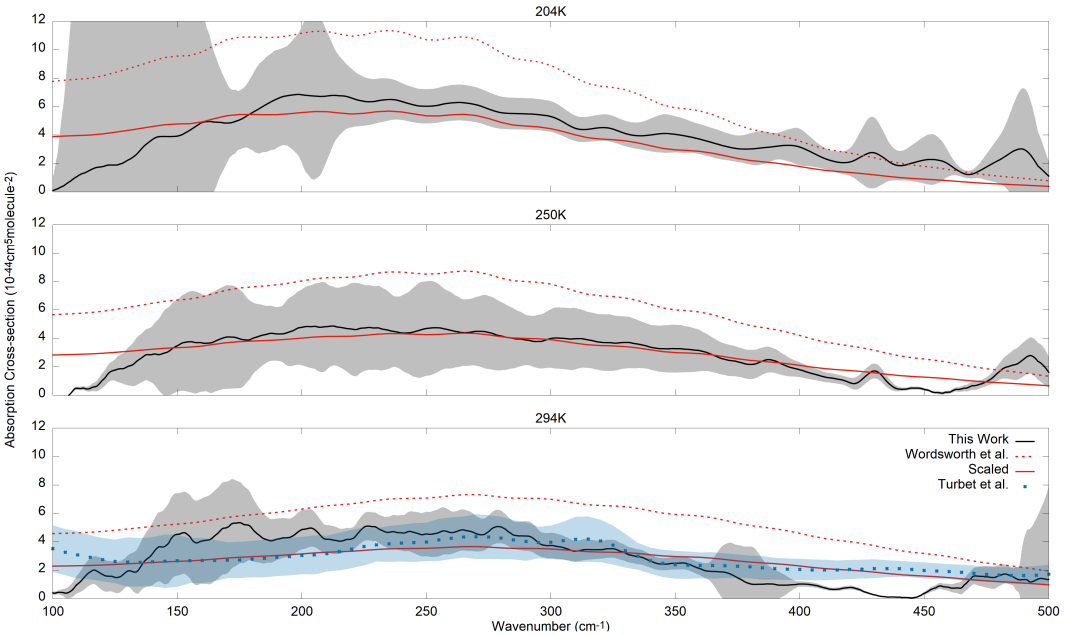

Figure 1: Experimental cross-section of CO_2-CH_4 CIA from this work (solid black line) along with comparisons to Wordsworth et al. (2017) (red dotted line), Wordsworth et al. (2017) prediction scaled by a factor of 0.5 (red solid line) to provide better agreement with the results from this work, and Turbet et al. (2019) measurement (blue X line). Uncertainty is represented by the shading around the experimentally derived measurements.

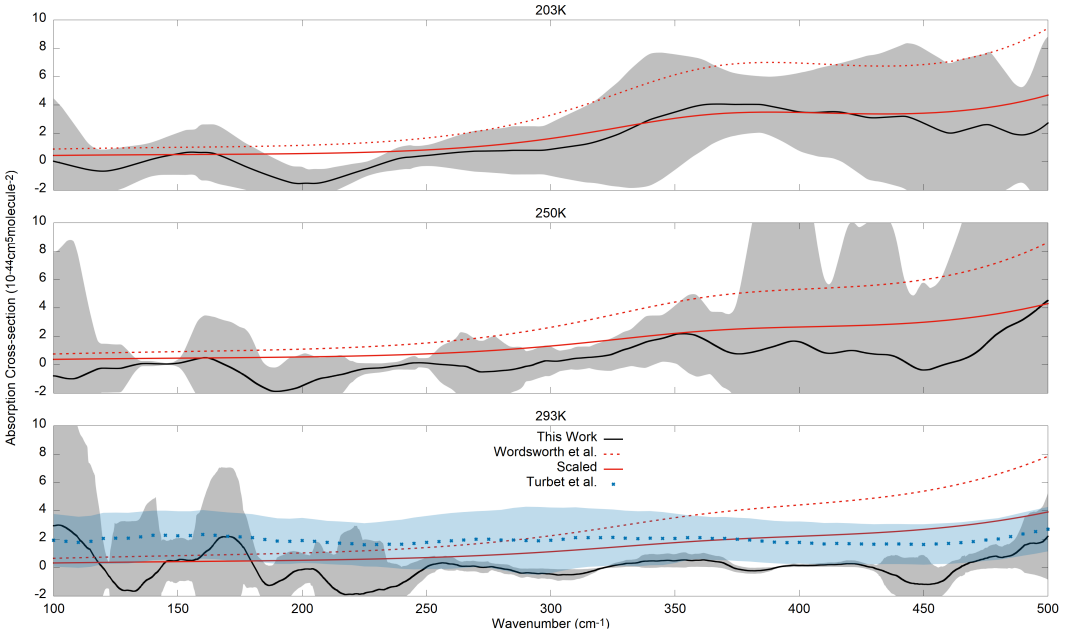

Figure 2: Experimental cross-section of CO_2-H_2 CIA from this work (solid black line) along with comparisons to Wordsworth et al. (2017) (red dotted line), Wordsworth et al. (2017) prediction scaled by a factor of 0.5 (red solid line) to provide better agreement with the results from this work, and Turbet et al. (2019) measurement (blue X line). Uncertainty is represented by the shading around the experimentally derived measurements.

3 Implications for Ancient Mars

3.1 Climate Model Details

Wordsworth et al. (2017) and Ramirez (Ramirez, 2017) investigated the effect on the ancient Martian climate by including the predicted CIA cross-sections in their radiative transfer models. However as noted in Section 2.2, there is a systematic overestimation in the predicted CIA for both CO_2-H_2 and CO_2-CH_4 by a factor of 2. Therefore, it is worth revisiting these climate calculations with experimentally verified CIA absorption values. Since the experimental CIA do not cover the full spectral range needed for radiative transfer modeling, it is assumed that the scaling factor of 2 needed to adjust the Wordsworth et al. (2017) CIA is consistent across the full spectral range. A scaled Wordsworth et al. (2017) CIA was used in a single-column radiative climate model following the same procedure as outlined below (Ramirez et al., 2014; Ramirez, 2017):

This model follows a moist adiabat at warmer temperatures and relaxes to a CO_2 adiabat when temperatures become cold enough for CO_2 to condense (Ramirez et al., 2014, 2014). The model uses the correlated-k technique to compute absorption for CO_2, H_2O, CH_4, and H_2 across 38 solar intervals, 55 infrared intervals, five temperatures (100, 200, 300, 400, and 600 K), and for eight pressures (10^{-5}–10^{2} bar). At the low temperatures considered here (<300 K), the HITRAN (Gordon et al., 2017) line list was utilized to compute k-coefficients at all wavelengths for CO_2 and H_2O, and in the thermal infrared for CH_4. The far wings of water vapor are modeled using the *Baranov Paynter Serio* (BPS) water vapor continuum (Paynter & Ramaswamy, 2011), which allows for accurately computed water vapor absorption at warm temperatures. However, the HITRAN line list is still incomplete for CH_4 at visible and near-infrared wavelengths (Kassi et al., 2008). Instead, near-infrared CH_4 k-coefficients for wavelengths under 1 micron from Karkoschka (Karkoschka, 1994) were combined with those from Irwin et al. (1996) for the spectral range between 1 and 4.5 microns. Rayleigh scattering for H_2O, CO_2, and CH_4 (Ramirez et al., 2014; Sneep & Ubachs, 2005) was included. CO_2-CH_4 and CO_2-H_2 CIA are incorporated, both from Wordsworth et al. (2017), and the CIA scaled by 0.5 to match the above experimental results. CO_2-CO_2 CIA is modeled following the procedure in Wordsworth et al. (2010), using experimental data from Baranov et al. (2004) and Gruszka and Borysow (1997).

Overall, the new CIA yield significantly cooler mean surface temperatures as shown in Figures 3a and 3b, when comparing the results from this work (solid lines) to the previous work (dashed lines). Mean surface temperatures above 273 K can be reached with the new CIA if surface pressures exceed ∼3 bar for a 10% CH_4 atmosphere. However, current studies on geologic observations suggest that the pressure on early Mars during valley network formation was no higher than ∼2 bar (Kite et al., 2014; Hu et al., 2015; Kurokawa et al., 2017). Another issue is that for CH_4 concentrations above a CH_4/CO_2 ratio of 0.1, photochemical hazes form that cool the planet, canceling the greenhouse effect (Haqq-Misra et al., 2008). Ultimately, CO_2-CH_4 absorption is not as promising as initially argued in Wordsworth et al. (Wordsworth et al., 2017). CO_2-H_2, however, still seems much more promising, as liquid water is possible with 5% hydrogen and less than 2 bar of surface pressure.

The planetary albedo plots are calculated here using the updated CIA and compared to those found in (Ramirez, 2017); as in that study, the planetary albedo decreases with increasing CH_4 or H_2 concentrations since this causes the overall atmospheric scattering to decrease. Comparing the effect of scaled versus unscaled CIA on planetary albedo, the albedo does not change significantly with the updated CIA for CO_2-CH_4 as shown in Figures 3c and 3d; this is primarily because water vapor amounts are still small at these temperatures. However with updated CO_2-H_2 CIA, there is a slight change in planetary albedo. This is because H_2 has a larger impact on the surface temperature (Figures 3a and 3b) compared to CH_4, which in turn increases the amount of water vapor in the atmosphere, resulting in the increased sensitivity of the planetary albedo to changes in CO_2-H_2 CIA. Additionally, atmospheres with CH_4 will have a lower planetary albedo than

those with H_2 is in part due to the increased absorption of CH_4 at solar wavelengths, which reduces the planetary albedo compared to H_2.

Following the analysis in (Ramirez, 2017), a comparison of temperature-altitude profiles for a fully-saturated 3 bar CO_2 early Mars atmosphere containing 1% CH_4 or 5% H_2 for a fully-saturated 2 bar CO_2 atmosphere were also performed using the updated CIA from this work. As seen in Figures 3e and 3f, there is little change in the temperature profile in the upper atmosphere when using Wordsworth et al. (2017) CIA or scaled CIA from this work; however at the surface there is $\sim$ 10 K difference in temperature.

4 Conclusions

This report details the first temperature-dependent experimental measurements of CO_2-H_2 and CO_2-CH_4 CIA. It was found that below 600 cm^{-1}, the experimentally derived CIA cross-sections agree with the spectral range and temperature dependence of the calculations by Wordsworth et al. (2017), however the amplitude is half of what was predicted. Furthermore, the CIA cross-sections reported here agree within combined uncertainty with those measured by Turbet et al. (2019), strengthening our confidence in these results.

With improved spectra, radiative transfer calculations of the early Mars atmosphere were performed and showed that CO_2-CH_4 CIA is not as promising as initially argued in Wordsworth et al. (Wordsworth et al., 2017) for producing a warm and wet early Mars. CO_2-H_2, however, still seems much more promising, as liquid water is possible with 5% hydrogen and less than 2 bar of surface pressure.

Acknowledgments

This work was supported by the Technologies for Exo-planetary Science (TEPS) Natural Sciences and Engineering Research Council of Canada (NSERC) CREATE Training Program. R. M. Ramirez acknowledges support from the Astrobiology Center (proposal grant number JY310064). The authors would like to thank Dr. Brant Billinghurst and Dr. Jianbao Zhao of the Far-IR beamline at the CLS for their assistance. Experimentally derived CIA cross-sections are available from the York University Dataverse repository: https://dataverse.scholarsportal.info/privateurl.xhtml?token=7d20f4c4-5fca-4d44-a2da-5dc42fa4db2b.

References

Abel, M., Frommhold, L., Li, X., & Hunt, K. L. C. (2011). Collision-induced absorption by h_2 pairs: From hundreds to thousands of kelvin. *J. Phys. Chem. A.*, *115*, 68056812. doi: 10.1021/jp109441f

Baranov, Y. I., Lafferty, W. J., & Fraser, G. T. (2004). Infrared spectrum of the continuum and dimer absorption in the vicinity of the o_2 vibrational fundamental in o_2/co_2 mixtures. *J. Mol. Spectrosc.*, *228*(2), 432440. doi: 10.1016/j.jms.2004

Barnhart, C. J., Howard, A. D., & Moore, J. M. (2009). Long-term precipitation and late-stage valley network formation: landform simulations of parana basin, mars. *J. Geophys. Res. Planets*, *114*(E01003). doi: 10.1029/2008JE003122

Borysow, A., & Frommhold, L. (1987). Collision-induced rototranslational absorption spectra of ch_4-ch_4 pairs at temperatures from 50 to 300 k. *Astrophys. J.*, *318*(940). doi: 10.1086/165426

Craddock, R. A., & Howard, A. D. (2002). The case for rainfall on a warm, wet early mars. *J. Geophys. Res. Planets*, *107*(5111). doi: 10.1029/2001JE001505

Gordon, I. E., Rothman, L. S., Hill, C., & *et al.* (2017). The hitran 2016 molecular spectroscopic database. *J. Quant. Spec. Rad. Trans.*, *203*, 3-69. doi: 10.1016/

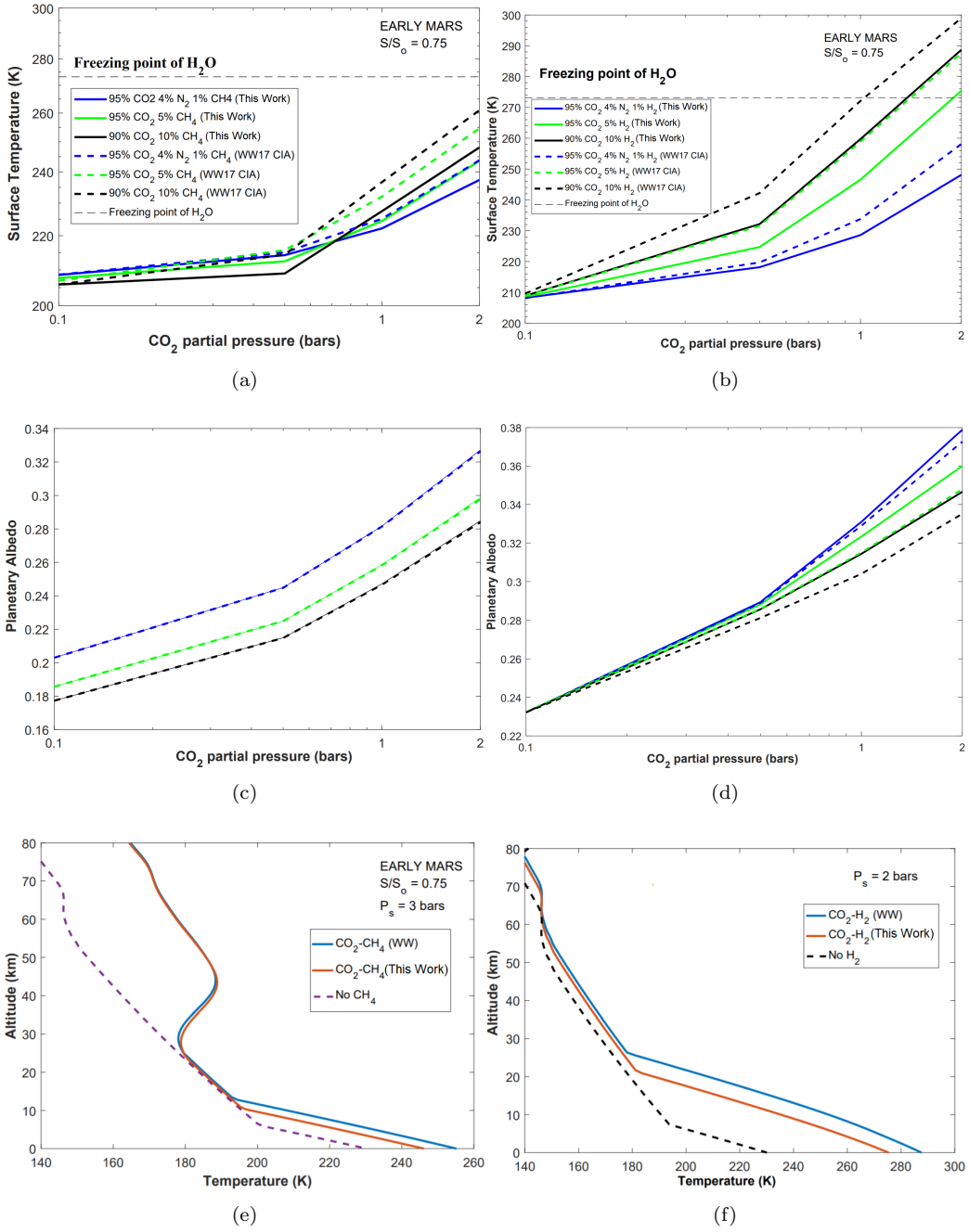

Figure 3: Early Mars climate modeling for atmospheres containing CH_4 or H_2. Dotted lines designate unscaled CIA from Wordsworth et al. (2017), while solid lines use CIA values scaled by 0.5. The model assumes that the effective stellar flux received by be Mars ∼4 billion years ago, is 75% of the present-day flux (S/S_O=0.75). First row: modeled surface temperature as a function of CO_2 partial pressure (log scale), at 1%, 5%, and 10% CH_4 (a) or H_2 (b). Second row: Mars' planetary albedo as a function of CO_2 partial pressure, at 1%, 5%, and 10% CH_4 (c) or H_2 (d). Third row: temperature-altitude profiles for a fully-saturated CO_2 early Mars atmosphere from Ramirez (2017) for atmospheres containing no CH_4 or H_2 (dashed line), 1% CH_4 (e) or 5% H_2 (f) using Wordsworth et al. (2017) CIA (blue line), and 1% CH_4 (e) or 5% H_2 (f) using CIA from this work (red line).

j.jqsrt.2017.06.038

Gruszka, M., & Borysow, A. (1997). Roto-translational collision-induced absorption of co_2 for the atmosphere of venus at frequencies from 0 to 250 cm^1, at temperatures from 200 to 800 k. *Icarus*, *129*(172). doi: 10.1006/icar.1997.5773

Haqq-Misra, J. D., Domagal-Goldman, S. D., Kasting, P. J., & Kasting, J. F. (2008). A revised, hazy methane greenhouse for the archean earth. *Astrobiology*, *8*(6), 1127-1137. doi: 10.1089/ast.2007.0197

Hu, R., Kass, D. M., Ehlmann, B. L., & Yung, Y. L. (2015). Tracing the fate of carbon and the atmospheric evolution of mars. *Nat. Commun.*, *6*(10003). doi: 10.1038/ncomms10003

Hynek, B. M., Beach, M., & Hoke, M. R. T. (2010). Updated global map of martian valley networks and implications for climate and hydrologic processes. *J. Geophys. Res. Planets*, *115*(E09008). doi: 10.1029/2009JE003548

Irwin, P. G. J., Calcutt, S. B., Taylor, F. W., & Weir, A. L. (1996). Calculated k distribution coefficients for hydrogenand self-broadened methane in the range 2000-9500 cm^{-1} from exponential sum fitting to band-modelled spectra. *J. Geo. Res. Planets*, *101*(E11), 26137-26154. doi: 10.1029/96JE02707

Karkoschka, E. (1994). Spectrophotometry of the jovian planets and titan at 300-to 1000-nm wavelength: The methane spectrum. *Icarus*, *111*(1), 174-192. doi: 10.1006/icar.1994.1139

Karman, T., Gordon, I. E., van der Avoird, A., Baranov, Y. I., Boulet, C., Drouin, B. J., ... van der Zande, W. J. (2019). Update of the hitran collision-induced absorption section. *Icarus*, *328*, 160-175. doi: 10.1016/j.icarus.2019.02.034

Kassi, S., Gao, B., Romaninia, D., & Campargue, A. (2008). The near-infrared (1.301.70 μm) absorption spectrum of methane down to 77 k. *Physical Chemistry Chemical Physics*, *10*(30), 4410-4419. doi: 10.1039/B805947K

Kite, E. S., Williams, J. P., Lucas, A., & Aharonson, O. (2014). Low palaeopressure of the martian atmosphere estimated from the size distribution of ancient craters. *Nat. Geosci.*, *7*, 335-339. doi: 10.1038/ngeo2137

Kochanov, R. V., Gordon, I. E., Rothman, L. S., Wciso, P., Hill, C., & Wilzewski, J. S. (2016). Hitran application programming interface (hapi): A comprehensive approach to working with spectroscopic data. *J. Quant. Spec. Rad. Trans.*, *177*, 15-30. doi: 10.1016/j.jqsrt.2016.03.005

Kurokawa, H., Kurosawa, K., & Usui, T. A. (2017). Lower limit of atmospheric pressure on early mars inferred from nitrogen and argon isotopic compositions. *Icarus*, *299*(1), 443-459. doi: 10.1016/j.icarus.2017.08.020

Mangold, N., Quantin, C., Ansan, V., Delacourt, C., & Allemand, P. (2004). Evidence for precipitation on mars from dendritic valleys in the valles marineris area. *Science*, *305*, 78-81. doi: 10.1126/science.1097549

Matsubara, Y., Howard, A. D., & Gochenour, J. P. (2013). Hydrology of early mars: valley network incision. *J. Geophys. Res. Planets*, *118*, 1365-1387. doi: 10.1002/jgre.20081

Paynter, D. J., & Ramaswamy, V. (2011). An assessment of recent water vapor continuum measurements upon longwave and shortwave radiative transfer. *J. Geo. Res. Atmospheres*, *116*(D20). doi: 10.1029/2010JD015505

Ramirez, R. M. (2017). A warmer and wetter solution for early mars and the challenges with transient warming. *Icarus*, *297*, 71-82. doi: 10.1016/j.icarus.2017.06.025

Ramirez, R. M., & Craddock, R. A. (2018). The geological and climatological case for a warmer and wetter early mars. *Nature Geoscience*, *11*(4), 230-237.

Ramirez, R. M., Kopparapu, R., Zugger, M. E., Robinson, T. D., Freedman, R., & Kasting, J. F. (2014). Warming early mars with co_2 and h_2. *Nature Geoscience*, *7*(1), 59. doi: 10.1038/ngeo2000

Sneep, M., & Ubachs, W. (2005). Direct measurement of the rayleigh scattering cross section in various gases. *J. Quant. Spec. Rad. Trans.*, *92*(3), 293-310. doi:

10.1016/j.jqsrt.2004.07.025

Stepinski, T. F., & Stepinski, A. P. (2005). Morphology of drainage basins as an indicator of climate on early mars. *J. Geophys. Res. Planets*, *110*(E12S12). doi: 10.1029/2005JE002448

Turbet, M., Tran, H., Pirali, O., Forget, F., Boulet, C., & Hartmann, J.-M. (2019). Far infrared measurements of absorptions by ch_4+co_2 and h_2+co_2 mixtures and implications for greenhouse warming on early mars. *Icarus*, *321*, 189-199. doi: 10.1016/j.icarus.2018.11.021

Wordsworth, R., Forget, F., & Eymet, V. (2010). Infrared collision-induced and far-line absorption in dense co_2 atmospheres. *Icarus*, *210*(2), 992-997. doi: 10.1016/j.icarus.2010.06.010

Wordsworth, R., Kalugina, Y., Lokshtanov, S., Vigasin, A., Ehlmann, B., Head, J., ... Wang, H. (2017). Transient reducing greenhouse warming on early mars. *Geophys. Res. Lett.*, *44*, 665-671. doi: 10.1002/2016GL071766